Journal of Integrative Agriculture 2020, 19(9): 2188–2205

Available online at www.sciencedirect.com

ScienceDirect

RESEARCH ARTICLE

Quantifying key model parameters for wheat leaf gas exchange under different environmental conditions

ZHAO Fu-nian[1, 2, 3], ZHOU Shuang-xi[4], WANG Run-yuan[3], ZHANG Kai[3], WANG He-ling[3], YU Qiang[1, 2, 5, 6]

[1] *Key Laboratory of Water Cycle & Related Land Surface Processes/Institute of Geographic Sciences and Natural Resources Research, Chinese Academy of Sciences, Beijing 100101, P.R.China*

[2] *College of Resources and Environment, University of Chinese Academy of Sciences, Beijing 100049, P.R.China*

[3] *Key Laboratory of Arid Climatic Change and Disaster Reduction of Gansu Province/Key Laboratory of Arid Climate Change and Disaster Reduction of China Meteorological Administration (CMA)/Lanzhou Institute of Arid Meteorology, CMA, Lanzhou 730020, P.R.China*

[4] *The New Zealand Institute for Plant and Food Research Limited, Hawke's Bay 4130, New Zealand*

[5] *State Key Laboratory of Soil Erosion and Dryland Farming on the Loess Plateau/Institute of Soil and Water Conservation, Northwest A&F University, Yangling 712100, P.R.China*

[6] *School of Life Sciences, University of Technology Sydney, Sydney 2000, Australia*

Abstract

The maximum carboxylation rate of Rubisco (V_{cmax}) and maximum rate of electron transport (J_{max}) for the biochemical photosynthetic model, and the slope (m) of the Ball-Berry stomatal conductance model influence gas exchange estimates between plants and the atmosphere. However, there is limited data on the variation of these three parameters for annual crops under different environmental conditions. Gas exchange measurements of light and CO_2 response curves on leaves of winter wheat and spring wheat were conducted during the wheat growing season under different environmental conditions. There were no significant differences for V_{cmax}, J_{max} or m between the two wheat types. The seasonal variation of V_{cmax}, J_{max} and m for spring wheat was not pronounced, except a rapid decrease for V_{cmax} and J_{max} at the end of growing season. V_{cmax} and J_{max} show no significant changes during soil drying until light saturated stomatal conductance (g_{ssat}) was smaller than 0.15 mol m^{-2} s^{-1}. Meanwhile, there was a significant difference in m during two different water supply conditions separated by g_{ssat} at 0.15 mol m^{-2} s^{-1}. Furthermore, the misestimation of V_{cmax} and J_{max} had great impacts on the net photosynthesis rate simulation, whereas, the underestimation of m resulted in underestimated stomatal conductance and transpiration rate and an overestimation of water use efficiency. Our work demonstrates that the impact of severe environmental conditions and specific growing stages on the variation of key model parameters should be taken into account for simulating gas exchange between plants and the atmosphere. Meanwhile, modification of m and V_{cmax} (and J_{max}) successively based on water stress

Received 8 April, 2019 Accepted 29 July, 2019
ZHAO Fu-nian, E-mail: zhaofn@iamcma.cn; Correspondence YU Qiang, E-mail: yuq@igsnrr.ac.cn

doi: 10.1016/S2095-3119(19)62796-6

severity might be adopted to simulate gas exchange between plants and the atmosphere under drought.

Keywords: biochemical photosynthetic model, stomatal conductance model, maximum carboxylation rate of Rubisco, maximum rate of electron transport, drought

1. Introduction

Gas exchange between leaf and the atmosphere plays a critical role for plant growth and survival in various environmental conditions (Kosugi and Matsuo 2006). It includes two main processes, the uptake of carbon dioxide from the atmosphere for photosynthesis and the release of water vapor from the plant for transpiration. These two processes are regulated by the aperture, or the conductance of stomas, on the leaf surface. However, multiple signal transduction mechanisms contribute to opening and closing of the aperture of stomas, involving both biochemical and biophysical aspects, and they are still not fully understood (Buckley and Mott 2013).

A large number of models have been commonly used in simulating stomatal conductance (Damour *et al*. 2010). Among others, the Ball-Berry (BB) Model (Ball *et al*. 1987) is the most commonly utilised empirical model. It estimates stomatal conductance (g_s) based on net photosynthesis (P_n), carbon dioxide (C_s) and relative humidity (RH_s) at the leaf surface. In the BB Model, C_s and RH_s can be easily obtained by meteorological factors and plant leaf characters, whereas the P_n can not be observed easily or calculated directly from meteorological data. Therefore, the Biochemical Photosynthetic Model for computing P_n (Farquhar *et al*. 1980) was adopted to couple with the BB Model for estimating gas exchange between plants and the atmosphere. The linking of these two models has proven to be hugely popular and has accurately simulated gas exchange for a large number of plant species at the leaf and canopy scales (Yu *et al*. 2002; Wang *et al*. 2006), as well as on regional and global scales (De Kauwe *et al*. 2015).

The maximum carboxylation rate of Rubisco (V_{cmax}) and maximum rate of electron transport (J_{max}) in the Biochemical Photosynthetic Model represent the intrinsic photosynthetic capacity of leaf (Egea *et al*. 2011). The slope (m) of the BB Model reflects a compromised relation between the benefits and costs of g_s relative to leaf photosynthetic activity (Ball *et al*. 1987). These three parameters are the most important model parameters for leaf gas exchange simulation. Misestimation of their values influences gas exchange simulation results greatly (Bauerle *et al*. 2014; Rogers 2014; Ali *et al*. 2015). Because it is time-consuming to obtain robust values by observation, these parameters have been mainly specified from literature and short-term measurements in field, pot or greenhouse. Meanwhile, identical and fixed values of these parameters have been used to simulate gas exchange in a large number of models for different species under various environmental conditions. However, their values vary not only with different species and functional types (Zhou *et al*. 2013), but also with diverse environmental conditions (Bunce 1998; Medlyn *et al*. 2002). At present, the great variation of biochemical photosynthetic model parameters and m for the BB Model between different species and plant functional types have been commonly accepted (Medlyn *et al*. 2002; Zhou *et al*. 2013; Miner *et al*. 2016). The impacts of environmental factors, such as temperature, carbon dioxide, water, and radiation, on these parameters also have been widely discussed (Bunce 1998; Muraoka *et al*. 2010; Ali *et al*. 2015; Miner and Bauerle 2017). However, the results of variation of these model parameters under different environmental conditions often disagree with each other. For example, several land surface models take m as a constant for plants under both well-watered and water deficit conditions, and they change V_{cmax} and J_{max} as drought develops (Sellers *et al*. 1996; Colello *et al*. 1998). On the contrary, a larger number of researchers suggest reducing m to simulate gas exchange between plant and the atmosphere as drought occurs (Beeck *et al*. 2010; Raab *et al*. 2015). Nevertheless, Xu and Baldocchi (2003) observed that m remained constant for blue oak during the whole growing season while severe water stress and extremely high air temperature affected the other two parameters, V_{cmax} and J_{max}.

Furthermore, a large number of previous researchers evaluated the effect of various environmental conditions on key model parameters, mainly focusing on trees (Baldocchi 1997; Xu and Baldocchi 2003; Osuna *et al*. 2015). Nevertheless, annual crops play critical roles in determining water and energy exchange between vegetation and the atmosphere in some areas of the world, especially in arid and semi-arid areas (Vote *et al*. 2015). Meanwhile, the life cycle of annual crops has unique characteristics. The whole growing season of annual crops is commonly limited to 1 year, and its morphological indexes might change greatly during a short period with different phenological stages (Ahuja *et al*. 2008). Recently, some crop models have used leaf gas exchange to simulate crop growth and yield formation, and to evaluate the effect of environmental factors on these processes taking global changes impact on crops into account (Fleisher *et al*. 2015; Masutomi *et al*. 2016; Seidel *et al*. 2016). This highlights the need for determining the variation of key model parameters of annual crops for accurate gas exchange simulation under different environmental conditions (Miner and Bauerle 2017, 2019).

Wheat (*Triticum aestivum* L.) is a typical annual crop, comprising the third largest crop in the world, and mainly grown in semi-humid, semi-arid and even some arid areas, under irrigation or totally rainfed condition (Wang *et al*. 2009). The prediction and quantification of carbon dioxide and water exchange for wheat cropland is very critical for agricultural water use and management in these areas. Hence, in this study, the leaf gas exchange of two wheat types during different growth stages under well-watered and drought conditions were measured. Meanwhile, a coupled model of the biochemical photosynthetic model and the BB Model was established. Our objectives were to: (1) quantify the variation of key parameters for the wheat leaf gas exchange model, V_{cmax}, J_{max} and m, under different wheat growth stages, different water supply conditions and diurnal changes of meteorological factors; and (2) evaluate the sensitivity of the coupled model to key parameters in simulating gas exchange under different meteorological conditions.

2. Materials and methods

2.1. Site description and experiments

The experiments for spring wheat were conducted in 2014, 2015 and 2017 at the Dingxi Arid Meteorology and Ecological Environment Field Experimental Station, Dingxi County of Gansu Province, Northwest China (35°33´N, 104°35´E, 1 896.7 m elevation). The site has a typical semi-arid climate with average annual precipitation of 386 mm (Zhao and Wang 2014; Zhao *et al*. 2018) for a full description of spring wheat growing conditions in the study region.

Spring wheat seeds were planted both in pots filled with 14 kg of air-dried soil and in the field in 2014 and 2017. In 2015, only the pot experiment was carried out. The spring wheat variety was Dingxixin 24 in all 3 years and it was sown in late March each year. For the pot experiments, 20 pots were sown with spring wheat, and 10 of these were randomly assigned to a well-watered treatment, the other 10 to a drought treatment. In 2014 and 2015, the different treatments were conducted during jointing stage and the drought treatment consisted of withholding water during the flowering period in 2017. Field experiments in 2014 had two water treatments, well-watered and drought, which were carried out during the jointing stage. In 2017, the field spring wheat was treated with two water supply conditions, one with enough water through the whole growth season and another under rainfed condition only. Air temperature, relative humidity (RH) and solar radiation were measured hourly at the experimental station.

The experiment for winter wheat was carried out at Yucheng Comprehensive Experiment Station (36°57´N, 116°36´E, 28 m elevation), Chinese Academy of Sciences, located in the North China Plain. Only one treatment was conducted at this station, winter wheat growing in the field with well-watered conditions. The experimental management and environmental conditions had been described by Yu *et al*. (2004) in detail.

2.2. Gas exchange measurements

Gas exchange for spring wheat was measured by two portable steady-state photosynthetic systems (Li-6400, Li-Cor Inc., Lincoln, NE, USA). Two types of response curve of P_n to photosynthetically active radiation (P_n/Q_p) and CO_2 concentration (P_n/C_i) were conducted in different years using a red-blue LED artificial light source (Table 1). Two first fully expanded leaves, with four replications, were selected to produce the response curves. For spring wheat, the P_n/Q_p curve was mainly monitored during the jointing stage (s2) in the pots and from the tillering stage (s1) to the milk stage (s6) in the field during 2014 and 2015. The P_n/C_i curve was produced in 2017 at the anthesis stage (s4) in the pots and from s1 to s6 in the field. For P_n/Q_p curves, wheat leaves were acclimated in the chamber with leaf temperature at 25°C and Q_p at 1 500 μmol m^{-2} s^{-1} for more than 40 min before making measurements. The Q_p used to generate the P_n/Q_p curves were 1 800, 1 500, 1 200, 900, 600, 300, 200, 120, 60, 30, 15, and 0 μmol m^{-2} s^{-1} while the CO_2 concentration was at a constant value, 400 μmol m^{-2} s^{-1}. Meanwhile, the measurement of P_n/Q_p curves under four different air temperatures (20, 25, 30, and 35°C) was conducted for spring wheat growing in the field during s2, to validate the coupling model. For production of P_n/C_i curves, before making measurements, wheat leaves were also acclimated in the chamber with a Q_p of 1 500 μmol m^{-2} s^{-1}, but two constant leaf temperatures at 25 and 30°C, were adopted, respectively. Then the CO_2 concentration was changed sequentially at 400, 200, 100, 50, 400, 600, 800, 1 000, and 1 200 μmol mol^{-1}. During measurement of the two types of curves, RH in the chamber was varied at (40±15)%. The minimum of 120 s and the maximum of 240 s were adopted respectively for individual measurements of each curve response to reach a steady state. Diurnal changes of gas exchange parameters for spring wheat under well-watered and rainfed conditions were monitored by Li-6400 with sunlight and free air conditions on 19 May in 2017 (day 57 after sowing, at s2). Three typical periods were

Table 1 Experimental information for leaf gas exchange observation of winter wheat and spring wheat growing in pots and the field for different years

Wheat type	Treatment		Year	Category of measurement[1)]	Stage[2)]
	Pot/Field	Well-watered/Drought			
Winter wheat	Field	Well-watered	2003	P_n/C_i	s2–s4
	Pot	Well-watered	2014, 2015	P_n/Q_p	s2
	Pot	Drought	2014, 2015	P_n/Q_p	s2
	Field	Well-watered	2014	P_n/Q_p	s1–s6
	Field	Drought	2014	P_n/Q_p	s4, s5
Spring wheat	Pot	Well-watered	2017	P_n/C_i	s3
	Pot	Drought	2017	P_n/C_i	s3
	Field	Well-watered	2017	P_n/C_i	s1–s6
	Field	Drought	2017	P_n/C_i	s4, s5, s6
	Field	Well-watered	2017	Sunlight	s3

[1)] P_n, net photosynthesis; C_i, intercellular CO_2; Q_p, photosynthetically active radiation.
[2)] s1, tillering stage; s2, jointing stage; s3, booting and heading stage; s4, anthesis stage; s5, grain-filling stage; s6, milk stage.

chosen to be analysed in this study, morning (08:00–11:00), noon (11:00–14:00) and afternoon (14:00–17:00).

At Yucheng Comprehensive Experiment Station, the P_n/C_i curve for winter wheat growing in the field under well-watered conditions was measured in approximately 1 week intervals, during late s2, whole booting and heading stages (s3) and early s4. The P_n/C_i curve was produced by the same approach for spring wheat under two controlled leaf temperatures, 25 and 30°C.

2.3. Calculation of model parameters and model validation

The coupling models and parameters for leaf gas exchange simulation are described and summarized in Appendices A and B. The input variables of the coupling models are radiation, temperature, RH, and CO_2 concentration and there are nine unknowns (P_n, g_s, leaf temperature (T_L), vapor pressure at the leaf surface (e_s), C_s, C_i, total water vapor conductance (g_v), heat conductance for boundary layer (g_h), and radiative conductance (g_r), refer to Appendix B). A nested iterative procedure was adopted to obtain these unknown variables numerically (Kim *et al*. 2003). The T_L was assumed to be equal to air temperature and C_i was at 0.7C_a firstly, and then used to estimate the P_n and g_s. The coupled mathematical model in this study was written and run by the computer programming language, Fortran90.

The P_n/C_i curve was used to estimate parameters V_{cmax} and J_{max}. As P_n was limited by Rubisco when C_i was less than 150 μmol mol^{-1}, V_{cmax} was estimated based on eq. (A2) in Appendix A. However, as P_n was limited by the regeneration of RuBP at higher C_i exposures, greater than 250 μmol mol^{-1}, J_{max} was determined by eqs. (A3) and (A4) in Appendix A. Furthermore, the data of the P_n/C_i curve collected during s2 to s4 were used for comparison of V_{cmax} and J_{max} under different temperatures between the two different wheat types.

To estimate the parameter m by eq. (A10) in Appendix A, we mainly used the data when Q_p was higher than 150 μmol m^{-2} s^{-1} and the CO_2 concentration greater than 100 μmol mol^{-1}, as recommended by previous researchers (Miner *et al*. 2016). For calculating m for winter wheat, the data of the P_n/C_i curve during s2 to early s4 were used. To compare the m values between winter wheat and spring wheat, the data of the P_n/C_i curve for spring wheat growing in the field in 2017 during s2 to s4 were used. The seasonal variation of m was calculated based on data of the P_n/Q_p curve for spring wheat growing in the field under well-watered conditions at s1, s2, s3, s4, grain-filling stage (s5), and s6. Photosynthetic parameters with Q_p at 1 500 μmol m^{-2} s^{-1} (defined as light saturated condition), temperature at 25°C and CO_2 at 400 μmol mol^{-1} from the P_n/Q_p curve in 2014 and 2015 and the P_n/C_i curve in 2017 for spring wheat both growing in pots and the field under different water conditions were used to calculate m. Hence, other environmental factors have relatively small impacts on m estimation under different water conditions.

The coupled model was tested by validation data sets. The data sets included the response of the main photosynthetic parameters, P_n, transpiration (T_r), g_s, and water use efficiency (WUE, P_n/T_r), to varied Q_p under four different ambient temperatures, 20, 25, 30, and 35°C.

2.4. Sensitivity analyses

Sensitivity analyses were conducted to determine the impact for variation of key model parameters (V_{cmax}, J_{max}, and m) on gas exchange simulation under diurnally meteorological conditions. Each parameter's effect was evaluated individually, and one parameter changed while other parameters were kept constantly. We chose a typical day in the Dingxi region during the spring wheat growing season and set each parameter to vary from a given value to –30% of it, and then compare the simulated results. Each parameter's effect (PE) was calculated as follows:

$$PE\ (\%)=(S_s-S_g)\times 100/S_g \quad (1)$$

where S_s is the simulated gas exchange parameters under 30% reduced key parameters and S_g is the simulated gas exchange parameters for a given key model parameter.

2.5. Redefinition of water supply condition

Due to the impact of different environmental conditions on drought occurrence, and adaptation strategies of plant to drought, plants would not suffer water stress immediately after withholding water supply. Therefore, we need to redefine water supply condition accurately for wheat in the current study. Medrano *et al*. (2002) suggested that g_s under light saturated condition (g_{ssat}) can be used as a reference of water stress indicator. Various water stress levels, mild, moderate, and severe, can be classified by g_{ssat} at 0.15 and 0.05 mol m^{-2} s^{-1} for C_3 crops (Cifre *et al*. 2005). In the current study, we adopted this approach instead of soil water content to divide spring wheat growing in pots and the field into two main water supply conditions. Spring wheat grown in pots and the field with g_{ssat} greater than 0.15 mol m^{-2} s^{-1} were defined as well-watered conditions (potww and fieldww). Spring wheat growing in pots and the field with g_{ssat} less than 0.15 mol m^{-2} s^{-1} were defined as water-stressed conditions (potdr and fielddr).

2.6. Statistical analyses

Non-linear regressions were used to calculate V_{cmax} and J_{max} and linear regressions were used to estimate m. The differences of V_{cmax} and J_{max} for spring wheat and winter wheat under different environmental conditions were tested by variance analysis. Linear, non-linear regressions and variance analysis were accomplished in R Software with functions of 'lm', 'nls', and 'TukeyHSD' (R Development Core Team 2014). Results were considered 'significant' as *P*-value less than 0.05. Before conducting statistical tests, data used in the study were examined to ensure homogeneity and normality of variances.

3. Results

3.1. Values of V_{cmax} and J_{max} for wheat

Comparison of V_{cmax} and J_{max} for winter wheat and spring wheat The average V_{cmax} for spring wheat at 25°C was about 95.9 μmol m^{-2} s^{-1}, *vs*. 107.5 μmol m^{-2} s^{-1} for winter wheat (Fig. 1-A), but there was no significant difference (*P*>0.05). As temperature increased, the V_{cmax} for both wheat types decreased significantly, and V_{cmax} was 76.1 μmol m^{-2} s^{-1} for spring wheat and 90.6 μmol m^{-2} s^{-1} for winter wheat at 30°C.

The average J_{max} values at 25°C were about 214.1 and 186.8 μmol m^{-2} s^{-1} for spring wheat and winter wheat, respectively (Fig. 1-B), and there was no significant difference. Meanwhile, J_{max} decreased for spring wheat and winter wheat as temperature increased to 30°C. However, there were no significant differences for J_{max} between the two temperatures for either wheat type.

Seasonal variation of V_{cmax} and J_{max} The V_{cmax} for spring wheat varied slightly from s1 to s5 and declined sharply at s6 (Fig. 2-A). The average V_{cmax} values for spring wheat were 93.1, 101.5, 95.1, 88.3, and 84.9 μmol m^{-2} s^{-1} at s1, s2, s3, s4, and s5, respectively. There were no significant differences of V_{cmax} among these stages. However, the V_{cmax} at s6, 78.2 μmol m^{-2} s^{-1}, was significantly lower than the value at s2.

The J_{max} for spring wheat at s1, s2, s3, s4, and s5 had no significant differences between them, whereas, J_{max}

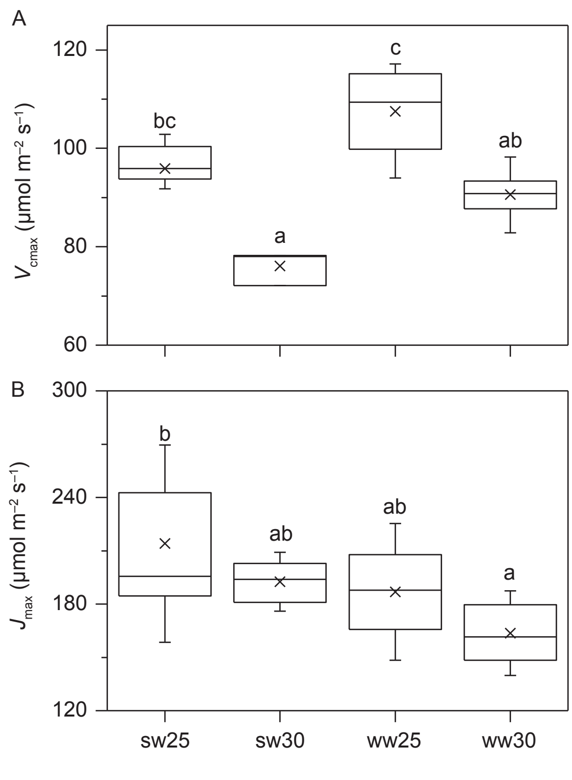

Fig. 1 Comparison of maximum carboxylation rate (V_{cmax}, A) and maximum electron transport capacity (J_{max}, B) under two different temperatures for well-watered spring wheat and winter wheat (*n*=3 to 10). sw25, spring wheat under 25°C. ww30, winter wheat under 30°C. Different lowercase letters indicate differences at 0.05 significance level with each treatment. The cross and horizontal lines inside each box are the average and median, respectively, the upper and lower end points of each box are the upper and lower quartile, respectively, and whiskers are the 1.5 times the interquartile ranges.

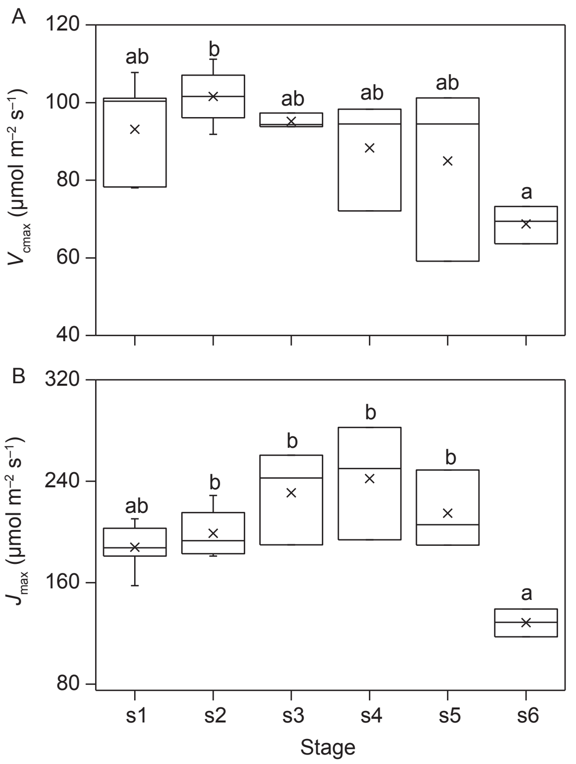

Fig. 2 Variation of maximum carboxylation rate (V_{cmax}, A) and maximum electron transport capacity (J_{max}, B) under different stages for well-watered spring wheat (n=3 to 5). s1–s6, tillering, jointing, booting, anthesis, grain-filling, and milk-ripe stages, respectively. Different lowercase letters indicate differences at 0.05 significance level with each treatment. The cross and horizontal lines inside each box are the average and median, respectively, the upper and lower end points of each box are the upper and lower quartiles, respectively, and whiskers are the 1.5 times the interquartile ranges.

at these five stages were significantly larger than at s6 (Fig. 2-B). Additionally, unlike the maximum V_{cmax} obtained at s2, the J_{max} at s4, 242.1 μmol m^{-2} s^{-1}, was larger than other five stages.

Variation of V_{cmax} and J_{max} under different water conditions The response of V_{cmax} to g_{ssat} both in the field and pot experiments, showed two totally different stages (Fig. 3-A). When g_{ssat} was greater than 0.15 mol m^{-2} s^{-1}, the V_{cmax} of spring wheat in the field showed no significant variation with the change of g_{ssat}, and it had a slightly decreasing trend for spring wheat in the pots (Table 2). Meanwhile, the statistical test of V_{cmax} for spring wheat grown in both pots compared with the field under well-watered conditions showed no significant difference (Fig. 3-B). However, when g_{ssat} was less than 0.15 mol m^{-2} s^{-1}, the V_{cmax} of spring wheat decreased sharply, especially for spring wheat growing in pots. Meanwhile, the average V_{cmax} for spring wheat at water-stressed conditions was significantly smaller than it was under well-watered conditions. Furthermore, the V_{cmax} for spring wheat growing in pots and the field were significantly different. The difference might be due to the spring wheat grown in the field suffering less severe water deficit compared with the pots.

Similarly, the variation of J_{max} for spring wheat growing in pots and the field against g_{ssat} fell into two apparently different stages, divided by g_{ssat} at 0.15 mol m^{-2} s^{-1} (Fig. 3-C). These J_{max} values changed slightly as g_{ssat} decreased from 0.6 to 0.15 mol m^{-2} s^{-1} (P>0.05) (Table 2), and there were no significant difference in J_{max} between spring wheat grown in pots and the field (Fig. 3-D). However, as g_{ssat} decreased from 0.15 to 0 mol m^{-2} s^{-1}, J_{max} of spring wheat both in the field and pots decreased significantly, and the average J_{max} values were significantly different from their values under well-watered condition.

Relationships between V_{cmax} and J_{max} As spring wheat developed, the J_{max}/V_{cmax} increased from 2.05 at s1 to 2.75 at s5, and declined sharply at s6, down to 1.88 (Fig. 4-A). However, there were no significant difference of J_{max}/V_{cmax} among these six stages.

There was no significant difference between J_{max}/V_{cmax} for winter wheat (1.77) and spring wheat (2.06) grown in the field under well-watered conditions (Fig. 4-B). However, the J_{max}/V_{cmax} for spring wheat grown in pots under well-watered conditions was 2.23, which was significantly larger than spring wheat grown in the field under well-watered condition. Meanwhile, when spring wheat suffered water deficit in both pots and the field, the J_{max}/V_{cmax} decreased. However, there was no significant difference of J_{max}/V_{cmax} for spring wheat under different water conditions, whether grown in pots or the field.

3.2. Values of m for the stomatal conductance model

Comparison of m for winter wheat and spring wheat The BB index (P_nRH/C_s) had a significant relationship with g_s for both wheat types, winter wheat and spring wheat grown in the field under well-watered conditions (Fig. 5). There was no significant difference between the m for winter wheat (12.172) and spring wheat (11.991) (Table 3). However, for a given BB index, the stomatal conductance of winter wheat was always slightly higher than that of the spring wheat. Combining the data of spring wheat and winter wheat, the m was 11.166 and g_o was 0.021 mol m^{-2} s^{-1}.

Seasonal variation of m for spring wheat At different growth stages for spring wheat under well-watered conditions, there was no apparent trend for the change of m (Fig. 6; Table 3). The m at s2 was 10.4, which was slightly higher than the values at s1, s3, s4, and s6, but with no significant differences. However, the m at s5 was 11.04, which had a significant difference with the slope in s6, 9.038. The overall m for spring wheat from s1 to s6 was 10.097,

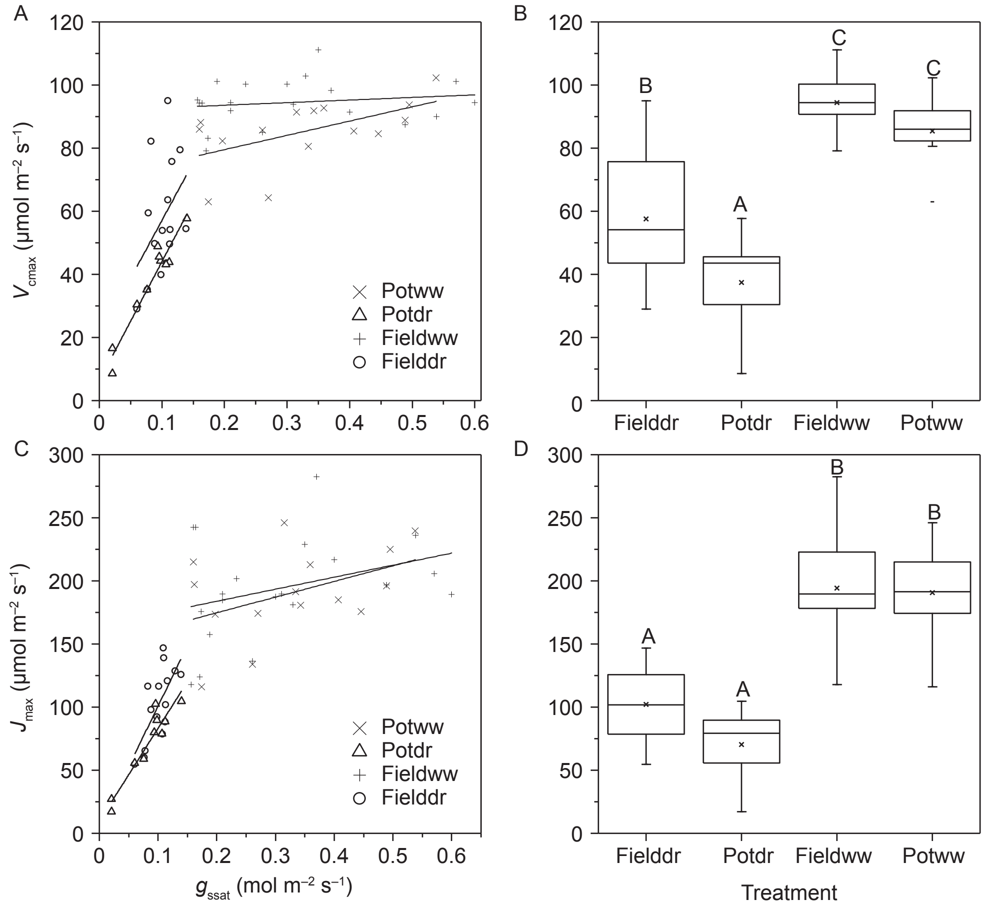

Fig. 3 Variation of maximum carboxylation rate (V_{cmax}, A and B) and maximum electron transport capacity (J_{max}, C and D) under different water conditions for spring wheat growing in pots and the field (n=10 to 19). Potww, spring wheat growing in pots with g_{ssat} greater than 0.15 mol m^{-2} s^{-1}; Potdr, spring wheat growing in pots with g_{ssat} less than 0.15 mol m^{-2} s^{-1}; Fieldww, spring wheat growing in the field with g_{ssat} greater than 0.15 mol m^{-2} s^{-1}; Fielddr, spring wheat growing in the field with g_{ssat} less than 0.15 mol m^{-2} s^{-1}. Different capital letters above or below the boxes indicate differences at 0.01 significance level with each treatment. The cross and horizontal line inside each box are the average and median, respectively, the upper and lower end points of each box are the upper and lower quartiles, respectively, and whiskers are 1.5 times the interquartile ranges.

Table 2 Response of maximum carboxylation rate of Rubisco (V_{cmax}) and maximum rate of electron transport (J_{max}) to light saturated stomatal conductance (g_{ssat}) under different water supply conditions

Variable	Growth condition[1)]	Slope	Intercept	R^2
V_{cmax}	Potww	45.224	70.482	0.308*
	Fieldww	–	–	–
	Potdr	377.332	6.294	0.934***
	Fielddr	–	–	–
	Potww+Fieldww	–	–	–
	Potdr+Fielddr	442.397	8.014	0.456***
J_{max}	Potww	–	–	–
	Fieldww	–	–	–
	Potdr	736.542	9.616	0.897***
	Fielddr	956.195	5.132	0.488**
	Potww+Fieldww	104.064	159.719	0.136*
	Potdr+Fielddr	891.936	5.709	0.672***

[1)] Potww, spring wheat growing in pots with g_{ssat} greater than 0.15 mol m^{-2} s^{-1}; Fieldww, spring wheat growing in the field with g_{ssat} greater than 0.15 mol m^{-2} s^{-1}; Potdr, spring wheat growing in pots with g_{ssat} less than 0.15 mol m^{-2} s^{-1}; Fielddr, spring wheat growing in the field with g_{ssat} less than 0.15 mol m^{-2} s^{-1}.

–, the significance level of the relation between V_{cmax} or J_{max} and g_{ssat} greater than 0.05, and the slope and intercept not shown. *, ** and ***, indicates signifcance level at 0.05, 0.01 and 0.001, respectively.

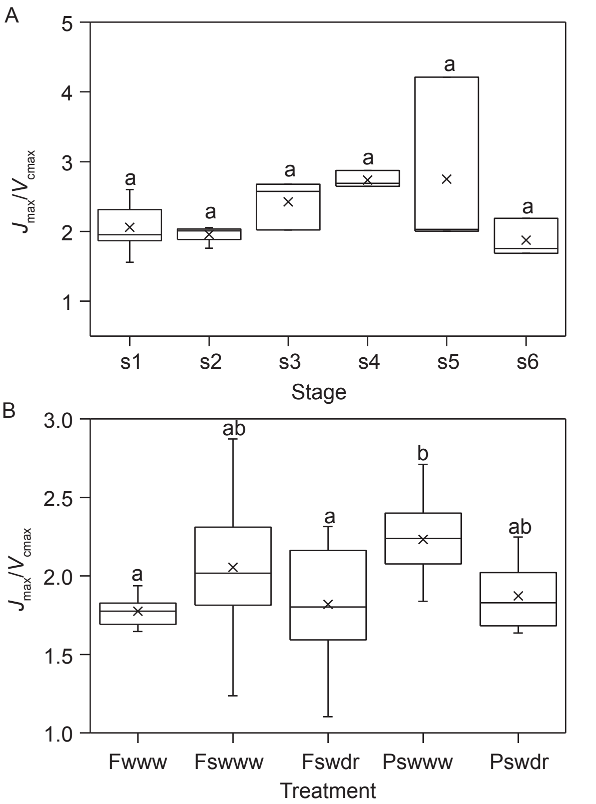

Fig. 4 Variation of ratios between maximum carboxylation rate (V_{cmax}) and maximum electron transport capacity (J_{max}) during different growth stages for spring wheat (A) and under different water condition for winter wheat and spring wheat (B). s1–s6, tillering, jointing, booting and heading, anthesis stage, grain-flling, and milk stages, respectively. Fwww, winter wheat growing in the field under well-watered condition; Fswww, spring wheat growing in the field under well-watered condition; Fswdr, spring wheat growing in the field under drought condition; Pswww, spring wheat growing in pots under well-watered condition; Pswdr, spring wheat growing in pots under drought condition. The same lowercase letters above or below boxes indicate no differences between each treatment. The cross and horizontal lines inside each box are the average and median of 3–19 individual measurements per treatment, respectively, the upper and lower end points of each box are the upper and lower quartile, respectively, and whiskers are 1.5 times the interquartile ranges.

and the g_0 was 0.038 mol m^{-2} s^{-1}.

Diurnal change of m for spring wheat The BB index had significant relationships with stomatal conductance at different times of the day for spring wheat growing in the field (Fig. 7-A). However, the m in the morning was 17.03, which was significantly higher than the values at noon and in the afternoon (Table 3). There was no significant difference between m at noon and in the afternoon. Meanwhile, the relationship between P_n and g_s was also significantly different at various time of the day (Fig. 7-B). The slope of P_n–g_s in the morning was significantly lower than the slope at noon and in the afternoon (Table 4). There was no significant difference of the P_n–g_s slope between noon and in the afternoon. We found leaf temperature in the morning was apparently lower than the temperature at noon and in the afternoon, and RH was higher than the value at noon and in the afternoon.

Variation of m for spring wheat under different water supply conditions There existed significant relationships between the BB index and g_{ssat} for spring wheat, when both grown in pots and the field under either well-watered or water-stressed conditions (Fig. 8-A). However, we found the m under well-watered condition was significantly greater than the value under water-stressed conditions (Table 3). The m was 10.6 and 10.8 in the field and pots under well-watered condition, respectively, whereas it was 7.5 and 6.9 under water-stressed condition in the field and pots, representing decreases of 29.7 and 36.3%, respectively. Combining the data of pots and the field, the m was 10.5 for well-watered spring wheat, *vs.* 7.3 under water-stressed conditions, a decrease of up to 31%.

As shown in Fig. 8-B and Table 4, the relationship between P_n and g_{ssat} for spring wheat under different water conditions was significantly different, both grown in pots and the field. The P_n–g_{ssat} slope under well-watered conditions was apparently lower than the slope under water-stressed conditions. There was no significant difference of the P_n–g_{ssat} slope between spring wheat growing in pots and the field both under well-watered and water-stressed conditions.

3.3. Parameter perturbation and sensitivity of gas exchange simulation

The comparison between observed gas exchange and simulated gas exchange showed the coupling model could simulate leaf gas exchange successfully (Appendix C). By using the model, key model parameters were perturbed individually, which consisted of altering the value of each parameter from given set of values (120 and 200 μmol m^{-2} s^{-1} and 12 for V_{cmax}, J_{max}, and m, respectively) to decreased them one-at-a-time by 30% while the others were kept constant. During a typical sunny day (Appendix C), the diurnal trends of P_n, T_r, g_s, and WUE with different key model parameters perturbation were nearly identical with the values calculated based on the given set of parameters (Fig. 9). However, it was shown that the values of P_n, T_r, g_s, and WUE were totally different from each other by parameter perturbation during the various time of the day.

For the 30% decreased value of V_{cmax}, the P_n was apparently lower than the normal treatment nearly all day (Fig. 9-A). The greatest difference, up to 30%, occurred at 11:00 as the P_n was at its maximum for the normal treatment during the day (Fig. 9-B). For T_r and g_s, V_{cmax} perturbation showed a slight decrease compared with the normal value (Fig. 9-C). The greatest difference occurred

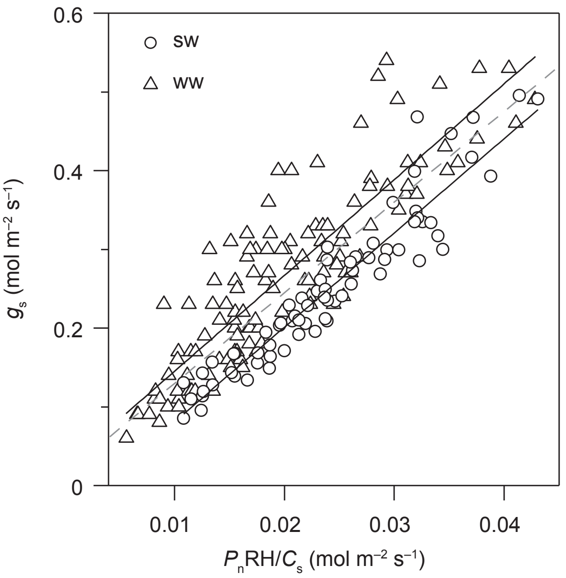

Fig. 5 Relationship between observed stomatal conductance (g_s) and the Ball-Berry Model index (P_nRH/C_s) for winter wheat and spring wheat under well-watered conditions from jointing to anthesis stages. sw, spring wheat; ww, winter wheat. P_n, net photosynthesis rate; RH, relative humidity; C_s, carbon dioxide.

later in the day, while T_r and g_s were at their maxima for the normal treatment, and the differences were not up to 30% (Fig. 9-C–F). Meanwhile, the perturbation of V_{cmax} showed nearly no effect on the diurnal variation of WUE (Fig. 9-G and H). The perturbation of J_{max} had nearly same effect on the variation of diurnal gas exchange at the perturbation of V_{cmax}. However, the differences between perturbed and normal values for P_n, T_r and g_s were slightly smaller than the difference of perturbation of V_{cmax} and the normal values, especially during the time from 10:00 to 18:00 (Fig. 9-A–F).

Compared with the perturbation of V_{cmax} and J_{max}, the decreased m value showed a very different effect on the diurnal variation of gas exchange. It decreased the P_n slightly as the normal treatment obtained the maximum P_n, but it had greater influence as P_n decreased in the afternoon (Fig. 9-A and B). The greatest difference for P_n between the normal and changed values of m occurred around noon. Meanwhile, perturbation of m had a great impact on the diurnal variation of T_r and g_s, and they decreased up to 30% nearly all day, sometimes even greater than 30% (Fig. 9-C–F). Furthermore, the decreasing of m apparently increased the WUE (Fig. 9-G and H), especially during the

Table 3 Variation of slope (m) and intercept (g_o) of Ball-Berry stomatal conductance model for winter wheat and spring wheat growing under different environmental conditions

Wheat type	Label[1)]	Stage	Growth condition		m	g_o	R^2
			Well-watered/Water-stressed	Pot/Field			
Spring wheat	sw	s2–s4	Well-watered	Field	11.991 a	–0.039	0.899***
Winter wheat	ww	s2–s4	Well-watered	Field	12.172 a	0.023	0.773***
Spring wheat+ Winter wheat	sw+ww	s2–s4	Well-watered	Field	11.166	0.021	0.731***
Spring wheat	sws1	s1	Well-watered	Field	9.451 ab	0.025	0.926***
	sws2	s2	Well-watered	Field	10.419 ab	–0.002	0.948***
	sws3	s3	Well-watered	Field	9.572 ab	0.064	0.735***
	sws4	s4	Well-watered	Field	9.044 ab	0.091	0.826***
	sws5	s5	Well-watered	Field	11.040 b	–0.010	0.942***
	sws6	s6	Well-watered	Field	9.038 a	0.103	0.751***
	s1–s6	s1–s6	Well-watered	Field	10.097	0.038	0.775***
Spring wheat	Fieldww	s2, s3, s4, s5	Well-watered	Field	10.645 B	0.010	0.774***
	Potww	s2, s4	Well-watered	Pot	10.837 B	–0.008	0.686***
	Fielddr	s4, s5	Water-stressed	Field	7.485 A	0.024	0.889***
	Potdr	s2, s4	Water-stressed	Pot	6.905 A	0.010	0.848***
	Potww+Fieldww	s2–s5	Well-watered	Field+Pot	10.688 B	0.0033	0.730***
	Potdr+Fielddr	s2, s4, s5	Water-stressed	Field+Pot	7.239 A	0.024	0.852***
	Potww+Fieldww+ Potdr+Fielddr	s2–s5	Well-watered+Water-stressed	Field+Pot	10.494	0.006	0.928***
Spring wheat	Morning	s3	Well-watered	Field	17.029 A	–0.048	0.836***
	Noon	s3	Well-watered	Field	12.702 B	0.017	0.979***
	Afternoon	s3	Well-watered	Field	11.564 B	0.036	0.910***
	All day	s3	Well-watered	Field	13.809	0.020	0.965***

[1)] sw, spring wheat; ww, winter wheat; s1–s6, tillering, jointing, booting and heading, anthesis, grain-flling, and milk stages, respectively. Fieldww, wheat growing in field under well-watered condition; Potww, wheat growing in pots under well-watered condition; Fielddr, wheat growing in field under drought condition; Potdr, wheat growing in pots under drought condition. Morning, observation at 08:00–11:00; noon, observation at 11:00–14:00; afternoon, observations at 14:00–17:00.

*** indicates significance level at 0.001. Different lowercase letters indicate differences at 0.05 significance level; different uppercase letters indicate differences at 0.01 significant level.

time from 07:00 to 12:00 when the g_s was relatively high.

4. Discussion

4.1. Variation of V_{cmax} and J_{max} for wheat under different conditions

The V_{cmax} of spring wheat and winter wheat under well-watered conditions at 25°C were nearly identical to those in previous reports, (88.14±6.3) to (108.44±8.2) μmol m^{-2} s^{-1} for four varieties wheat of Katarina *et al*. (2016), for instance. The J_{max} of spring wheat and winter wheat under well-watered conditions at 25°C were in the range of seasonal variation for winter wheat reported in Sun *et al*. (2015), although they took mesophyll conductance into account when calculating V_{cmax} and J_{max}. Meanwhile, we found the photosynthesis rate for wheat under well-watered conditions in the current study was higher than in most trees (Sala and Tenhunen 1996), and so was the V_{cmax} and J_{max} (Kosugi and Matsuo 2006). However, as the V_{cmax} and J_{max} for wheat were comparable with the maximum values of blue oak (Xu and Baldocchi 2003); the P_{nmax} (net photosynthesis rate obtained under saturating Q_p) of blue oak at the time with the highest V_{cmax} and J_{max} was nearly identical to the values in this study, i.e., g_{ssat} approached 0.5 mol m^{-2} s^{-1} in Fig. 8. This finding clearly confirmed the close relationship between biochemical parameters and P_{nmax}, and higher photosynthetic capability of the plants indicates a higher photosynthesis rate. Furthermore, it also verifies the fact that the P_{nmax} could be used to determine key model parameters, V_{cmax} and J_{max} (Xu and Baldocchi 2003; De Kauwe *et al*. 2016), if one lacks of the equipment or enough time to measure the P_n/C_i curve.

Temperature greatly affects the variation of V_{cmax} and J_{max}, which has been found by previous studies (Medlyn *et al*. 2002; Hikosaka *et al*. 2006). The optimal temperature for wheat growth ranges from 19 to 23°C (Slafer and Rawson 1995). As the temperature increased to 30°C, it significantly decreased V_{cmax} for wheat compared with its value at 25°C. Meanwhile, we found the V_{cmax} and J_{max} in our study

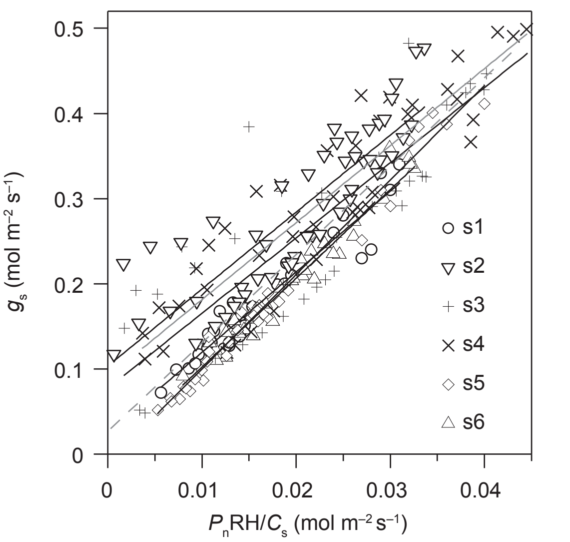

Fig. 6 Relationship between observed stomatal conductance (g_s) and the Ball-Berry Model index (P_nRH/C_s) for spring wheat during different growth stages. P_n, net photosynthesis rate; RH, relative humidity; C_s, carbon dioxide.

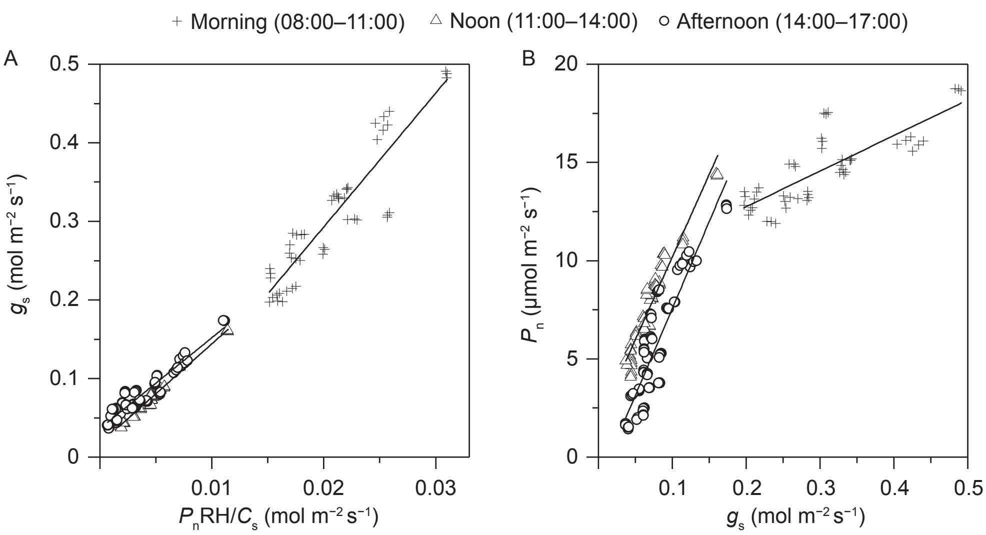

Fig. 7 Diurnal variation of the relationship between observational stomatal conductance (g_s) and the Ball-Berry Model index (P_nRH/C_s) (A) and relationship between P_n and g_s (B) for spring wheat. The slopes of the BB Model were significantly different between morning and noon. P_n, net photosynthesis rate; RH, relative humidity; C_s, carbon dioxide.

Table 4 Relationships between light saturated stomatal conductance (g_{ssat}) and net photosynthesis rate (P_n) under different times and different water conditions for spring wheat growing in pots and the field

Label[1)]	Growth condition		Slope	Intercept	R^2	T_{leaf} (°C)	Q_p (μmol m^{-2} s^{-1})	RH (%)	CO_2 (μmol mol^{-1})
	Well-water/Water-stress	Pot/Field							
Morning	Well-watered	Field	18.111 A	9.125	0.652***	22±1	1 600±100	50±5	400±10
Noon	Well-watered	Field	84.106 B	1.775	0.927***	33±2	1 800±50	27±3	400±10
Afternoon	Well-watered	Field	88.486 B	–1.287	0.820***	31±2	1 400±100	28±4	400±10
Fielddr	Water-stressed	Field	115.163 B	–0.049	0.818***	25±2	1 500±5	40±10	400±5
Fieldww	Well-watered	Field	28.419 A	10.69	0.720***	25±2	1 500±5	50±10	400±5
Potdr	Water-stressed	Pot	114.623 B	–0.380	0.936***	25±2	1 500±5	40±10	400±5
Potww	Well-watered	Pot	19.086 A	13.999	0.473***	25±2	1 500±5	50±10	400±5

[1)] All numbers of XX±YY represent the maximum and minimum of leaf temperature (T_{leaf}), photosynthetically active radiation (Q_p), relative humidity (RH), and CO_2 concentration (CO_2), respectively.
*** indicates significance level at 0.001. Different uppercase letters indicate differences at 0.01 significant level.

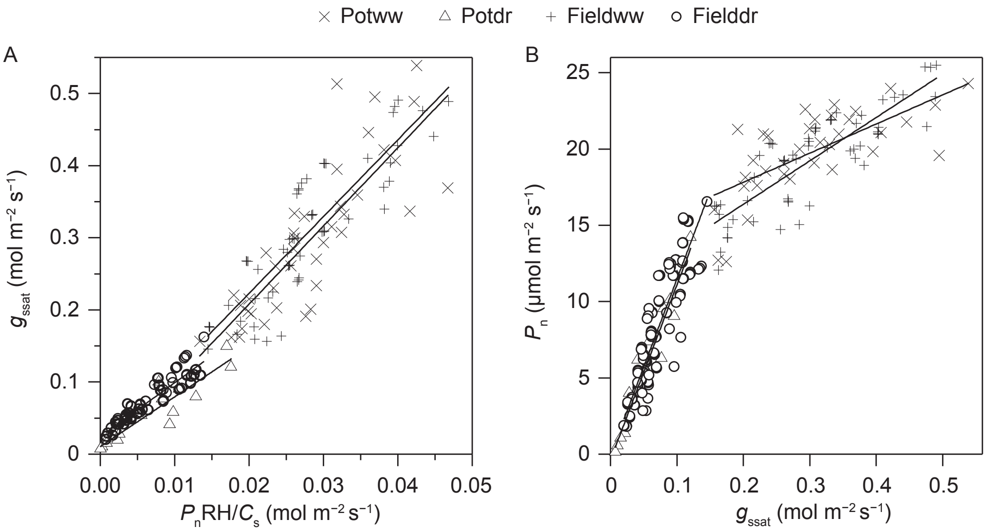

Fig. 8 Variation of relationship between observed light saturated stomatal conductance (g_{ssat}) and the Ball-Berry Model index (P_nRH/C_s) (A) and relationship between net photosynthesis rate (P_n) and g_{ssat} (B) for spring wheat grown in pots and the field under different water conditions. P_n, net photosynthesis rate; RH, relative humidity; C_s, carbon dioxide. Potww, wheat growing in pots under well-watered condition; Potdr, wheat growing in pots under drought condition; Fieldww, wheat growing in field under well-watered condition; Fielddr, wheat growing in field under drought condition.

were slightly lower than the values obtained by Driever *et al*. (2014) for 64 field-grown wheat genotypes under a leaf temperature of 20°C. Taking the range of optimal temperatures for wheat into account, we speculated that the differences in the two parameters between our study and Driever *et al*. (2014) is not only due to the diversity of photosynthetic capacity among wheat varieties, but also the temperature effect.

Although the trend in the data is similar to the results from other studies (Medlyn *et al*. 2002; Xu and Baldocchi 2003; Bauerle *et al*. 2012), the seasonal variation of V_{cmax} and J_{max} for spring wheat did not significantly fluctuated. The exception was a sharp reduction at the end of the growth season, which was identical with the results reported by Grossman *et al*. (1999). Several researchers have speculated that the seasonal variation in V_{cmax} might be related to leaf ontogeny, water stress, temperature and Rubisco specific activity (Grassi *et al*. 2005; Iio *et al*. 2008; Urban *et al*. 2012). Meanwhile, others have suggested that the biochemical model parameters are tightly correlated with leaf nitrogen content or nitrogen use efficiency (Ali *et al*. 2015; Tatsumi *et al*. 2019). The duration of the whole growth season for spring wheat in the current research was only 110 days. With enough nitrogen supply at planting time, there would be no nitrogen deficit for spring wheat compared with winter wheat, which has a longer growth season, generally more than 200 days. The nitrogen could be transferred from old leaves to new leaves as the wheat grows. Therefore, there might have been great variation in V_{cmax} and J_{max} for winter wheat leaves during different growth stages in other studies (Feng *et al*. 2015; Sun *et al*. 2015). Meanwhile, Rubisco content has an inverse

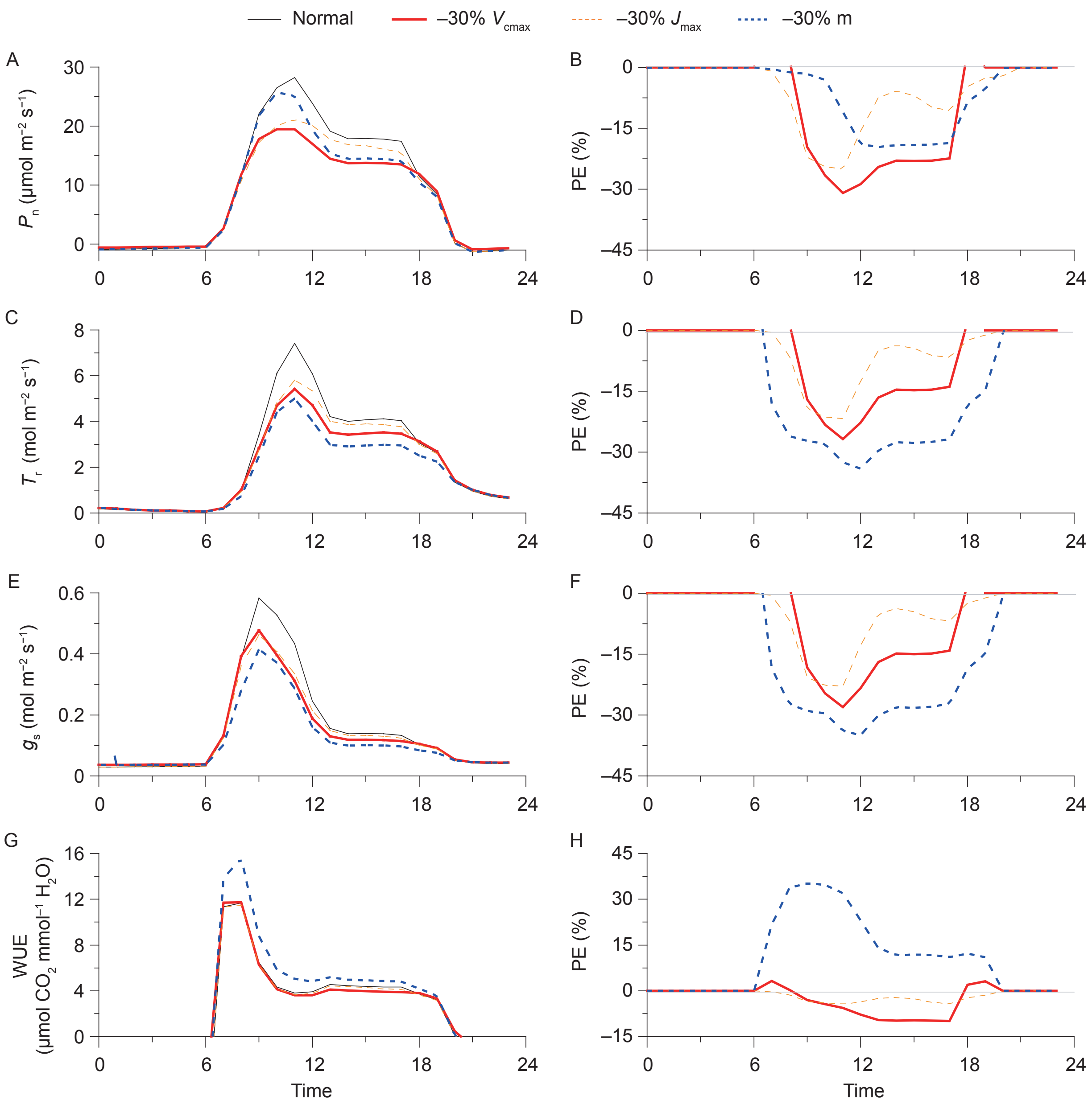

Fig. 9 Effects of variable key model parameters on diurnal leaf gas exchange for spring wheat. V_{cmax}, the maximum carboxylation rate of Rubisco; J_{max}, the maximum rate of electron transport. P_n, net photosynthesis; PE, parameters effect; T_r, transpiration rate; g_s, stomatal conductance; WUE, water use efficiency.

relationship with its specific activity (Urban *et al*. 2012). The increase of Rubisco specific activity that accompanies its content decrease might offset the reduction of V_{cmax} and J_{max} during the middle-late growing season for spring wheat. Furthermore, a group of studies have found that photoperiod could result in seasonal variation of V_{cmax} and J_{max} (Bauerle *et al*. 2012; Way *et al*. 2017). The main growing season for spring wheat is from April to June. The longer day length in June might prevent the down-regulation of V_{cmax} and J_{max} at the middle-late growing season for spring wheat. It should be noted also that the observation of seasonal V_{cmax} and J_{max} for spring wheat in the current study was conducted under well-watered conditions with strict environmental control, and, thus, without water and temperature stress. Therefore, the fluctuation of seasonal V_{cmax} and J_{max} for spring wheat was not pronounced, except at the end of the growing season with leaf senescence and a sharp reduction of leaf nitrogen content (Grossman *et al*. 1999).

Water deficit has significant impacts on the biochemical parameters of the photosynthetic model. However, it did not affect the model parameters until the water stress progressed to a specific threshold, g_{ssat} at 0.15 mol m^{-2}

s^{-1} in the current study. Previous studies have found that biochemical limitation for photosynthesis only occurs under moderate to severe water deficit condition (Brodribb 1996; Medrano *et al*. 2002). We speculated that spring wheat only suffered mild water stress before g_{ssat} approached 0.15 mol m^{-2} s^{-1} in the current study and the stomatal conductance decreased without V_{cmax} and J_{max} being reduced in proportion. Meanwhile, in the field experiment, the g_{ssat} was relatively higher, therefore, the V_{cmax} was significantly higher than the wheat growing in pots, which suffered an extremely severe water stress at the end of the observation period, as g_{ssat} approached zero.

Previous studies have reported mean J_{max}/V_{cmax} ranging from 1.6 to 1.7 for a large number of plant species, and it was shown to be sensitive to changes in environmental factors (Medlyn *et al*. 2002). We noted that the J_{max}/V_{cmax} for spring wheat under well-watered condition was slightly higher than those reported by Osuna *et al*. (2015) and Medlyn *et al*. (2002) for tree species. This indicates that spring wheat may allocate more nitrogen to electron transport than to Rubisco, which could be an optimal strategy for spring wheat in the study area, which has high radiation for spring wheat growth. However, more research is certainly warranted on this topic.

4.2. Variation of m under different conditions

The m values for the two wheat types during s2 to s4 in the current study were nearly identical with each other, and comparable with the results obtained in Lei *et al*. (2011) for winter wheat in the middle of the growing season. However, the m was higher than the commonly used value for C_3 plant in several land surface models, e.g., nine in Simple Biosphere Model 2 (SiB2) (Sellers *et al*. 1997). The land surface models always adopts an average value for C_3 plants, despite the fact that great variation exists in the m values for different C_3 plants, 13.3±10 (Miner *et al*. 2016). This variation suggests that species differences of m should be taken into account as we simulate the gas exchange of various plants.

Some previous researchers have stated that the relationship between g_s and the BB index remained constant both under water-stressed and well-watered conditions (Wong *et al*. 1979, 1985). In contrast, a large number of studies have modified the m by multiplying it by a water stress coefficient, to make the simulated gas exchange more comparable with observations (Baldocchi 1997; Liu *et al*. 2009). In the current research, we found that the m for spring wheat had two significantly different values under different water conditions, which could be divided by g_{ssat} at 0.15 mol m^{-2} s^{-1}. Due to the strict environment at controls used in the current study (Table 4), the only factor affecting the variation of m was water. Meanwhile, we found that the P_n and g_{ssat} relationship was also affected by different water conditions (Fig. 8-B), which was identical to the previous statement that water deficit could modify the relationship between P_n and g_s, and consequently the g_s–P_n ratio (Bunce 1998; Damour *et al*. 2010). In the studies of Wong *et al*. (1979, 1985), they found the P_n and g_s varied in proportion even under mild water-stressed conditions, and the ratio of C_i and C_a remained constant. Nevertheless, in our study, we found that the slope of P_n–g_s apparently increased under drought conditions, to nearly three times that of well-watered wheat. Meanwhile, the C_i/C_a was not a constant, but decreased with g_s and then increased sharply

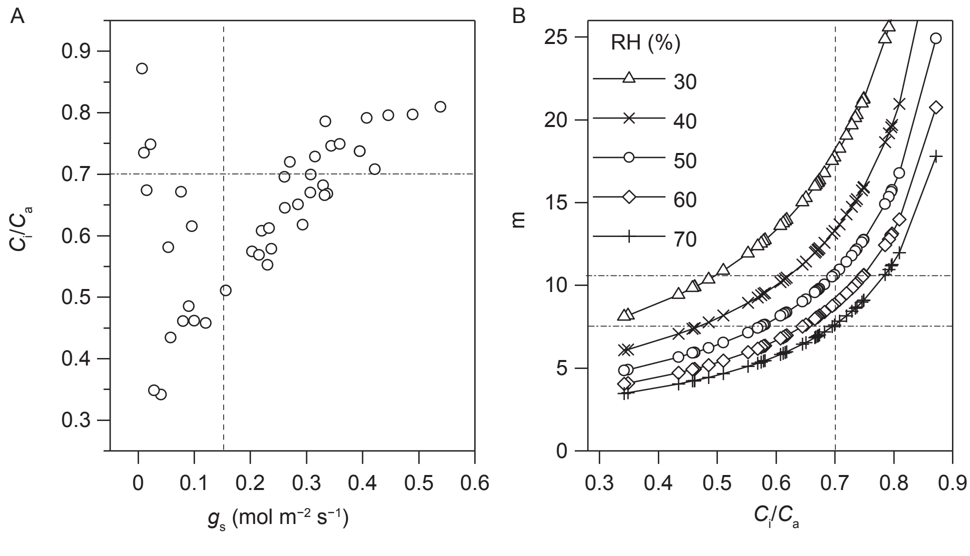

Fig. 10 The variation of the ratio of intercellular CO_2 to atmospheric CO_2 (C_i/C_a) for spring wheat grown in pots under different water conditions (A) and response of the slope (m) to variation C_i/C_a under different relative humidities (RH) (B).

as g_s became smaller than 0.05 mol m^{-2} s^{-1} (Fig. 10-A). P_n can be calculated as follows:

$$P_n=\frac{g_s}{1.6}C_a(1-C_i/C_a) \quad (2)$$

If C_i/C_a is constant and C_a is at a fixed value, then the relation between P_n and g_s would not change and m could remain constant even when water stress occurs. However, as the relationship between P_n and g_s changes, the m might vary. We took the derivative of eq. (A10) in Appendix A and eq. (2), and obtained the following eq.:

$$m=\frac{1.6}{RH(1-C_i/C_a)} \quad (3)$$

This reflects that the m is determined both by the RH and C_i/C_a (Fig. 10-B). Given a fixed RH, 50% for instance, we calculated the m for C_3 and C_4 plants to be 10.7 and 5.3, respectively, as the mean C_i/C_a for C_3 and C_4 plant were 0.7 and 0.4, respectively (Wong *et al*. 1979). The calculated m for C_3 and C_4 plants are nearly identical to the values most often used in several land surface models, nine for C_3 and four for C_4 plants (Sellers *et al*. 1997). In the current research, the RH for the well-watered condition was 50%, and 40% for the water-stressed condition (Table 4). The average C_i/C_a for well-watered spring wheat was 0.7 and it was 0.45 for water-stressed wheat, if we neglect the sharply increased C_i/C_a, where we speculated the impairment of the photosynthesis apparatus occurred (Brodribb 1996). Therefore, we obtained the m for spring wheat under well-watered and drought conditions from Fig. 10-B, 10.2 and 7.1, respectively. We found the values from the figures were nearly identical to the values obtained from the linear relationships in Table 3, 10.6 and 7.3, respectively. In the study of Xu and Baldocchi (2003), they showed there was no difference in m under different water supply conditions. However, they obtained the m without controlling the ambient temperature, and the RH would be very low with temperatures up to 33°C as seasonal drought occurred in their study. Fig. 10-B shows that the m would be higher if RH is low, even with small C_i/C_a. We speculate this might be the reason that some researchers found m had not decreased under water-stressed condition.

The environmental conditions during different growth stages or different times of the day have an effect on m. Ono *et al*. (2013) found m was higher during early and late growing seasons for rice. Lei *et al*. (2011) showed the m remained nearly constant at first, but rapidly increased at the end of the winter wheat growing season. In the study of Lei *et al*. (2011), the m was calculated based on data from daily observations with skylights for radiation and without temperature control. However, under identical meteorological conditions for observations in the current study, the m varied slightly and nearly remained constant with the development of spring wheat, except in s5 when m was higher than the other stages. Meanwhile, we found the m calculated during different time of the day with skylights for radiation and without temperature control were not identical, especially a higher value was obtained in the morning. Shimono *et al*. (2010) also found that m for irrigated rice varied diurnally, with an especially lower value in the afternoon. The relationships between P_n and g_s in the current study were totally different in the morning, at noon and in the afternoon (Fig. 7-B), which contrast with Ball (1987), who found a constant relationship of g_s and P_n with no influence of meteorological factors. In our study, we found the environmental factors, leaf temperature and RH at noon and in the afternoon, were apparently higher and lower than in the morning, respectively. A previous study had verified that increasing vapor pressure deficit, which is calculated from temperature and RH, results in C_i/C_a decreasing (Kemanian *et al*. 2005). Based on eq. (3), with variation of RH and C_i/C_a, m might vary diurnally. Furthermore, these two meteorological factors might induce greater variation of P_n at noon and in the afternoon compared with in the morning with the same change of g_s (Fig. 7-B), which also represents an adjustment of the relationship between P_n and g_s, hence, a change of m.

Decreased m indicates that plants adopt a more conservative water use strategy. Therefore, it could increase intrinsic water use efficiency (IWUE, P_n/g_s) (Egea *et al*. 2011), to maximize carbon gain while minimizing water loss (De Miguel *et al*. 2012). This might be a very efficient approach for a crop to escape environmental stress, such as high temperature, low relative humidity and water deficit. As the plant grows under optimal conditions, the m would increase to a maximum value, in the morning and under well-watered conditions in the current study, for instance. Under such conditions, the plant could accumulate more dry matter without taking water loss into account.

4.3. Implications for coupling models to simulate gas exchange

Because of no significant differences among key model parameters between spring wheat and winter wheat, it has been suggest that we could use these parameters obtained from references to simulate gas exchange for wheat during main growth season under favorable environmental conditions, if we do not have experimental data to calculated these parameters directly. However, it should be noted that a limited understanding of model parameterization could result in much uncertainty of the carbon and water cycle estimates at different scales. At the leaf scale, we found the variation of key model parameters, V_{cmax}, J_{max} and m, had totally different impacts on gas exchange with variable meteorological conditions, which were consistent with the finding of Bauerle *et al*. (2014) at the canopy scale. Due to the significant decrease of model parameters under water-stressed, high temperature, large vapor pressure deficit conditions and late growing season, the variation of key model parameters under both severe environmental conditions and specific growing stages should be taken into account, to simulate gas exchange between plants and the atmosphere accurately.

What processes limit P_n under drought is still under debate. Generally, the variation of m and V_{cmax} (and J_{max}) are related to stomatal and non-stomatal factors influencing photosynthetic process (Keenan *et al*. 2010). Hence, modification of m or V_{cmax} (and J_{max}) are commonly adopted for simulating gas exchange under drought (Egea *et al*. 2011). However, accounting for water stress in a coupling model by modification of m or V_{cmax} (and J_{max}) separately has failed to represent the variation of several observed key leaf gas exchange attributes during drought, especially IWUE (Egea *et al*. 2011). In field experiments, plant leaf IWUE always increases as water stress develops (Limousin *et al*. 2010), and we speculate that decreased m could capture this phenomenon in the gas exchange estimate (eq. (4), derived from eq. (A10) in Appendix A with neglect of g_o).

$$\text{IWUE}=\frac{P_n}{g_s}=\frac{C_s}{\text{mRH}} \tag{4}$$

However, IWUE decreased with water stress up to a threshold in field experiments (Medrano *et al*. 2009). This might indicate that m stops increasing at a specific water stress degree and never approaches to zero, resulting in IWUE approaching infinity, which is verified in our research in Fig. 10-B. The non-stomatal factors would limit photosynthetic process greatly as severe drought occurs (V_{cmax} and J_{max} decreased while g_{ssat} was less than 0.15 mol m^{-2} s^{-1} in the current study), which might result in P_n and IWUE decreasing sharply (Medrano *et al*. 2002; Egea *et al*. 2011). These results suggest that we could modify m and V_{cmax} (and J_{max}) successively based on water stress severity to simulate gas exchange under drought.

5. Conclusion

Meteorological factors and water supply conditions greatly affect the variation of key model parameters for wheat leaf exchange, including V_{cmax}, J_{max} and m. However, there were no significant differences for V_{cmax}, J_{max} and m between spring wheat and winter wheat. Meanwhile, the seasonal variation of V_{cmax}, J_{max} and m for spring wheat was not obvious, except a rapid decrease for V_{cmax} and J_{max} at maturity. The study demonstrates that environmental factors alter key parameter values of ecological models over specific growing stages, which should be taken into account for simulating gas exchange between plants and the atmosphere.

Acknowledgements

This research was jointly supported by the National Natural Science Foundation of China (41375019, 41730645, and 41275118) and the China Special Fund for Meteorological Research in the Public Interest (Major projects) (GYHY201506001-2).

Appendices associated with this paper can be available on http://www.ChinaAgriSci.com/V2/En/appendix.htm

References

Ahuja L R, Saseendran S A, Reddy V R, Yu Q. 2008. Synthesis, actions, and further research to improve response of crop system models to water stress. In: Ahuja L R, Reddy V R, Saseendran S A, Yu Q, eds., *Response of Crops to LimitedWater*: *Understanding and Modeling Water Stress Effects on Plant Growth Processes*. American Society of Agronomy, Crop Science Society of America, Soil Science Society of America, Madison WI. pp. 411–422.

Ali A A, Xu C, Rogers A, Fisher R A, Wullschleger S D, Massoud E C, Vrugt J A, Muss J D, McDowell N G, Fisher J B, Reich P B, Wilson C J. 2015. A global scale mechanistic model of the photosynthetic capacity. *Geoscientific Model Development Discussions*, **8**, 6217–6266.

Baldocchi D D. 1997. Measuring and modelling carbon dioxide and water vapour exchange over a temperate broad-leaved forest during the 1995 summer drought. *Plant Cell and Environment*, **209**, 1108–1122.

Ball J T, Woodrow I E, Berry J A. 1987. A model predicting stomatal conductance and its contribution to the control of photosynthesis under different environmental conditions. In: *Progress in Photosynthesis Research 7th International Congress*. Martinus Nijhoff Publishers, Biggins. pp. 221–224.

Bauerle W L, Daniels A B, Barnard D M. 2014. Carbon and water flux responses to physiology by environment interactions: A sensitivity analysis of variation in climate on photosynthetic and stomatal parameters. *Climate Dynamics*, **42**, 2539–2554.

Bauerle W L, Oren R, Way D A, Qian S S, Stoy P C, Thornton P E, Bowden J D, Hoffman F M, Reynolds R F. 2012. Photoperiodic regulation of the seasonal pattern of photosynthetic capacity and the implications for carbon cycling. *Proceedings of the National Academy of Sciences of the United States of America*, **109**, 8612–8617.

Beeck M D, Löw M, Deckmyn G, Ceulemans R. 2010. A comparison of photosynthesis dependent stomatal models using twig cuvette field data for adult beech (*Fagus sylvatica* L.). *Agricultural and Forest Meteorology*, **150**, 531–540.

Brodribb T. 1996. Dynamics of changing intercellular CO_2

concentration (C_i) during drought and determination of minimum functional C_i. *Journal of Plant Physiology*, **111**, 179–186.

Buckley T N, Mott K A. 2013. Modelling stomatal conductance in response to environmental factors. *Plant Cell and Environment*, **36**, 1691–1699.

Bunce J A. 1998. Effects of environment during growth on the sensitivity of leaf conductance to changes in humidity. *Global Change Biology*, **4**, 269–274.

Cifre J, Bota J, Escalona J M. 2005. Physiological tools for irrigation scheduling in grapevine (*Vitis vinifera* L.): An open gate to improve water-use efficiency? *Agricultural Ecosystem Environment*, **106**, 159–170.

Colello G D, Grivet C, Sellers P J, Berry J A. 1998. Modeling of energy, water and CO_2 flux in a temperate grassland ecosystem with SiB2: May to October 1987. *Journal of Atmoshere Science*, **55**, 1141–1169.

Damour G, Simonneau T, Cochard H, Urban L. 2010. An overview of models of stomatal conductance at the leaf level. *Plant*, **33**, 1419–1438.

Driever S M, Lawson T, Andralojc P J, Raines C M, Parry A J. 2014. Natural variation in photosynthetic capacity, growth, and yield in 64 field-grown wheat genotypes. *Journal Experimental Botany*, **65**, 4959–4973.

Egea G, Verhoef A, Vidale P L. 2011. Towards an improved and more flexible representation of water stress in coupled photosynthesis-stomatal conductance models. *Agricultural and Forest Meteorology*, **151**, 1370–1384.

Farquhar G D, Von C S, Berry J A. 1980. A biochemical model of photosynthetic CO_2 assimilation in leaves of C_3 species. *Planta*, **149**, 78–90.

Feng Z Z, Pang J, Kobayashi K, Zhu J, Ort D R. 2015. Differential responses in two varieties of winter wheat to elevated ozone concentration under fully open-air field conditions. *Global Change Biology*, **17**, 580–591.

Fleisher D H, Dathe A, Timlin D J, Reddy V R. 2015. Improving potato drought simulations: Assessing water stress factors using a coupled model. *Agricultural and Forest Meteorology*, **200**, 144–155.

Grassi G, Vicinelli E, Ponti F, Cantoni L, Magnani F. 2005. Seasonal and interannual variability of photosynthetic capacity in relation to leaf nitrogen in a deciduous forest plantation in northern Italy. *Tree Physiology*, **25**, 349–360.

Grossman C S, Kimball B A, Hunsaker D J, Long S P, Garcia R L,Kartschall T, Wall G W, Printer P J, Wechsung F, LaMorte R L. 1999. Effects of elevated atmospheric CO_2 on canopy transpiration in senescent spring wheat. *Agricultural and Forest Meteorology*, **93**, 95–109.

Hikosaka K, Ishikawa K, Borjigidai A, Muller O, Onoda Y, Atkin O K, Borland A M, Hodge A. 2006. Temperature acclimation of photosynthesis: Mechanisms involved in the changes in temperature dependence of photosynthetic rate. *Journal of Experiemental Botany*, **57**, 291–302.

Iio A, Yokoyama A, Takano M, Nakamura T, Fukasawa H, Nose Y, Kakubari Y. 2008. Interannual variation in leaf photosynthetic capacity during summer in relation to nitrogen, leaf mass per area and climate within a *Fagus crenata* crown on Naeba Mountain, Japan. *Tree Physiology*, **28**, 1421–1432.

Katarina O, Marek K, Marian B, Marek Z, Pavol S, Bo S H. 2016. Genotypically identifying wheat mesophyll conductance regulation under progressive drought stress. *Frontiers in Plant Science*, **7**, 1–14.

De Kauwe M G, Kala J, Lin Y S, Pitman A J, Medlyn B E, Duursma R A, Abramowitz G, Wang Y P, Miralles D G. 2015. A test of an optimal stomatal conductance scheme within the CABLE land surface model. *Geoscience Model Development*, **8**, 431–452.

De Kauwe M G, Lin Y S, Wright I J, Medlyn B E, Crous K Y, Ellsworth D S, Maire V, Prentice I C, Atkin O K, Rogers A, Niinemets U, Serbin S P, Meir P, Uddling J, Togashi H F, Tarvainen L, Weerasinghe L K, Evans B J, Ishida F Y, Domingues T F. 2016. A test of the 'one-point method' for estimating maximum carboxylation capacity from field-measured, light-saturated photosynthesis. *New Phytologist*, **210**, 1130–1144.

Keenan T, Sabate S, Gracia C. 2010. Soil water stress and coupled photosynthesis-conductance models: Bridging the gap between conflicting reports on the relative roles of stomatal, mesophyll conductance and biochemical limitations to photosynthesis. *Agricultural and Forest Meteorology*, **150**, 440–453.

Kemanian A R, Stöckle C O, Huggins D R. 2005. Transpiration-use efficiency of barley. *Agricultural and Forest Meteorology*, **130**, 1–11.

Kim S H, Lieth J H. 2003. A coupled model of photosynthesis, stomatal conductance and transpiration for a rose leaf (*Rosa hybrida* L.). *Annal of Botany*, **91**, 771–781.

Kosugi Y, Matsuo N. 2006. Seasonal fluctuations and temperature dependence of leaf gas exchange parameters of co-occurring evergreen and deciduous trees in a temperate broad-leaved forest. *Tree Physiology*, **26**, 1173–1184.

Lei H M, Yang D W, Shen Y, Liu Y, Zhang Y. 2011. Simulation of evapotranspiration and carbon dioxide flux in the wheat-maize rotation croplands of the North China Plain using the Simple Biosphere Model. *Hydrology Process*, **25**, 3107–3120.

Limousin J M, Misson L, Lavoir A V, Martin N K, Rambal S. 2010. Do photosynthetic limitations of evergreen quercus ilex leaves change with long-term increased drought severity? *Plant Cell and Environment*, **33**, 863–875.

Liu F L, Andersen M N, Jensen C R. 2009. Capability of the 'Ball-Berry' model for predicting stomatal conductance and water use efficiency of potato leaves under different irrigation regimes. *Scientia Horticulturae*, **122**, 346–354.

Masutomi Y, Ono K, Mano M, Maruyama A, Miyata A. 2016. A land surface model combined with a crop growth model for paddy rice (MATCRO-Rice v.1) Part I: Model description. *Geoscience Model Development Discussions*, **9**, 4133–4154.

Medlyn B E, Dreyer E, Ellsworth D, Forstreuter M, Harley P C, Kirschbaum M U F, Roux X L, Montpied P, Strassemeyer J, Walcroft A. 2002. Temperature response of parameters of a biochemically based model of photosynthesis. II. A review of experimental data. *Plant Cell and Environment*, **25**, 1167–1179.

Medrano H, Escalona J M, Bota J, Gulías J, Flexas J. 2002. Regulation of photosynthesis of C_3 plants in response to progressive drought: Stomatal conductance as a reference parameter. *Annals of Botany*, **89**, 895–905.

Medrano H, Flexas J, Galmés J. 2009. Variability in water use efficiency at the leaf level among Mediterranean plants with different growth forms. *Plant and Soil*, **317**, 17–29.

De Miguel M, Sanchez G D, Cervera M T, Aranda I. 2012. Functional and genetic characterization of gas exchange and intrinsic water use efficiency in a full-sib family of *Pinus pinaster* Ait. in response to drought. *Tree Physiology*, **32**, 94–103.

Miner G L, Bauerle W L. 2017. Seasonal variability of the parameters of the Ball-Berry model of stomatal conductance in maize (*Zea mays* L.) and sunflower (*Helianthus annuus* L.) under well-watered and water-stressed conditions. *Plant Cell and Environment*, **40**, 1874–1886.

Miner G L, Bauerle W L. 2019. Seasonal responses of photosynthetic parameters in maize and sunflower and their relationship with leaf functional traits. *Plant Cell and Environment*, **42**, 1561–1574.

Miner G L, Bauerle W L, Baldocchi D D. 2016. Estimating the sensitivity of stomatal conductance to photosynthesis: A review. *Plant Cell and Environment*, **40**, 1214–1238.

Muraoka H, Saigusa N, Nasahara K N, Noda H, Yoshino J, Saitoh T M, Nagai S, Murayama S, Koizumi H. 2010. Effects of seasonal and interannual variations in leaf photosynthesis and canopy leaf area index on gross primary production of a cool-temperate deciduous broadleaf forest in Takayama, Japan. *Journal of Plant Research*, **123**, 563–576.

Ono K, Maruyama A, Kuwagata T, Mano M, Takimoto T, Hayashi K, Hasegawa T, Miyata A. 2013. Canopy-scale relationships between stomatal conductance and photosynthesis in irrigated rice. *Global Change Biology*, **19**, 2209–2220.

Osuna L J, Baldocchi D D, Kobayashi H, Dawson E T. 2015. Seasonal trends in photosynthesis and electron transport during the Mediterranean summer drought in leaves of deciduous oaks. *Tree Physiology*, **35**, 485–500.

R Development Core Team. 2014. R: A language and environment for statistical computing, Vienna, Austria. [2015-05-06]. https://www.r-project.org/

Raab N, Meza F J, Franck N, Bambach N. 2015. Empirical stomatal conductance models reveal that the isohydric behavior of an Acacia caven Mediterranean Savannah scales from leaf to ecosystem. *Agricultural and Forest Meteorology*, **213**, 203–216.

Rogers A. 2014. The use and misuse of V_{cmax} in earth system models. *Photosynthesis Research*, **119**, 15–29.

Sala A, Tenhunen J D. 1996. Simulations of canopy net photosynthesis and transpiration in *Quercus ilex* L. under the influence of seasonal drought. *Agricultural and Forest Meteorology*, **78**, 203–222.

Seidel S J, Rachmilevitch S, Schütze N, Lazarovitch N. 2016. Modelling the impact of drought and heat stress on common bean with two different photosynthesis model approaches. *Environmental Modelling Software*, **81**, 111–121.

Sellers P J, Dickinson R E, Randall D A, Betts A K, Hall F G, Berry J A, Collatz G J, Denning A S, Mooney H A, Nobre C A. 1997. Modeling the exchanges of energy, water, and carbon between continents and the atmosphere. *Science*, **275**, 502–509.

Sellers P J, Randall D A, Collatz G J, Berry J A, Field C B, Dazlich D A, Zhang C, Collelo G D, Bounoua L. 1996. A revisedland surface parameterization (SiB2) for atmospheric GCMs. Part I: Model formulation. *Journal of Climate*, **9**, 676–705.

Shimono H, Masumi O, Meguru I, Hirofumi N, Kazuhiko K, Hasegawa T. 2010. Diurnal and seasonal variations in stomatal conductance of rice at elevated atmopheric CO_2 under fully open-air conditions. *Plant Cell and Environment*, **33**, 322–331.

Slafer G A, Rawson H M. 1995. Base and optimum temperatures vary with genotype and stage of development in wheat. *Plant Cell and Environment*, **18**, 671–679.

Sun J, Sun J, Feng Z Z. 2015. Modelling photosynthesis in flag leaves of winter wheat (*Triticum aestivum* L.) considering the variation in photosynthesis parameters during development. *Functional Plant Biology*, **42**, 1036–1044.

Tatsumi K, Kuwabara Y, Motorayashi T. 2019. Monthly variability in the photosynthetic capacities, leaf mass per area and leaf nitrogen contents of rice (*Oryza sativa* L.) plants and their correlations. *Journal of Agricultural Meteorology*, **75**, 111–119.

Urban O, Hrstka M, Zitová M, Holiová P, Mirka P, Sprtova M, Klem K, Calfapietra C, Angelis P D, Marek M V. 2012. Effect of season, needle age and elevated CO_2 concentration on photosynthesis and rubisco acclimation in *Picea abies*. *Plant Physiology and Biochemistry*, **58**, 135–141.

Vote C, Hall A, Charlton P. 2015. Carbon dioxide, water and energy fluxes of irrigated broad-acre crops in an Australian semi-arid climate zone. *Environmental Earth Sciences*, **73**, 449–465.

Wang F H, He Z H, Sayre K, Li S D, Si J S, Feng B, Kong L G. 2009. Wheat cropping systems and technologies in China. *Field Crop Research*, **111**, 181–188.

Wang J, Yu Q, Li J, Li L H, Li X G, Yu G R, Sun X M. 2006. Simulation of diurnal variations of CO_2, water and heat fluxes over winter wheat with a model coupled photosynthesis and transpiration. *Agricultural and Forest Meteorology*, **137**, 194–219.

Way D A, Stinziano J R, Berghoff H, Oren R, Cernusak L. 2017. How well do growing season dynamics of photosynthetic capacity correlate with leaf biochemistry and climate fluctuations? *Tree Physiology*, **37**, 1–10.

Wong S C, Cowan I R, Farquhar G D. 1979. Stomatal conductance correlates with photosynthetic capacity.

Nature, **282**, 424–426.
Wong S C, Cowan I R, Farquhar G D. 1985. Leaf conductance in relation to rate of CO_2 assimilation. III. Influences of water stress and photoinhibition. *Journal of Plant Physiology*, **78**, 830–834.
Xu L K, Baldocchi D D. 2003. Seasonal trends in photosynthetic parameters and stomatal conductance of blue oak (*Quercus douglasii*) under prolonged summer drought and high temperature. *Tree Physiology*, **23**, 865–877.
Yu Q, Liu Y Q, Liu J D, Wang T D. 2002. Simulation of leaf photosynthesis of winter wheat on Tibetan Plateau and in North China Plain. *Ecology Modelingl*, **155**, 205–216.
Yu Q, Zhang Y G, Liu Y F, Shi P L. 2004. Simulation of the stomatal conductance of winter wheat in response to light, temperature and CO_2 changes. *Annals of Botany*, **93**, 435–441.
Zhao F N, Lei J, Wang R Y, Zhang K, Wang H L, Yu Q. 2018. Determining agricultural drought for spring wheat with statistical models in a semi-arid climate. *Journal of Agricultural Meteorology*, **74**, 162–172.
Zhao F N, Wang R Y. 2014. Discrimination of drought occurrence for rainfed spring wheat in semi-arid area based on pattern recognition. *Transactions of the Chinese Society of Agricultural Engineering*, **30**, 124–132.
Zhou S X, Duursma R A, Medlyn B E, Kelly J W G, Prentice I C. 2013. How should we model plant responses to drought? An analysis of stomatal and non-stomatal responses to water stress. *Agricultural and Forest Meteorology*, **182**, 204–214.

Executive Editor-in-Chief LI Shao-kun
Managing editor WANG Ning